The interaction of CO_2 concentrations and water stress in semi-arid areas causes diverging response in instantaneous water use efficiency and carbon isotope composition

Na Zhao[1], Ping Meng[2], Yabing He[1], Xinxiao Yu[1]*

[1] College of soil and water conservation, Beijing Forestry University, Beijing 100083, P.R. China
[2] Research Institute of Forestry, Chinese Academy of Forestry 100091, Beijing, P.R. China

Abstract. In the context of global warming attributable to the increasing levels of CO_2, severe drought can be anticipated in areas with chronic water shortages (semi-arid areas), which necessitates research on the interaction between elevated atmospheric concentrations of CO_2 and drought on plant photosynthetic discrimination. The ^{13}C fractionation may be generated through the transformation from photosynthate to sugars before transporting them outward the leaf. The influence of environmental conditions (i. e. CO_2 concentration and water stress) and their interactions on this fractionation have not yet been identified. Therefore, saplings of species typical to a semi-arid area of Northern China that have similar growth status—*Platycladus orientalis* and *Quercus variabilis*—were selected and cultivated in growth chambers with orthogonal treatments (four CO_2 concentrations [CO_2] $\times$ five soil volumetric water contents (SWC)). The $\delta^{13}C$ of water-soluble compounds extracted from leaves of potted saplings was measured to determine the instantaneous water use efficiency (WUE_{cp}) after cultivation. Instantaneous water use efficiency derived from gas exchange (WUE_{ge}) was integrated to estimate differences in $\delta^{13}C$ signal variation before leaf-exported translocation of primary assimilates. The WUE_{ge} of the two saplings both decreased with increased soil moisture, and increased with elevated [CO_2] at 35%–80% of Field Capacity (FC) by strengthening photosynthetic capacity and reducing transpiration. Differences in instantaneous water use efficiency (iWUE) according to distinct environmental changes differed between the species. The WUE_{ge} of *P. orientalis* was significantly greater than that of *Q. variabilis*, while the opposite results were obtained in a comparison of the WUE_{cp} of the two species. Total ^{13}C fractionation from the site of carboxylation to cytoplasm before sugars transportation (total ^{13}C fractionation) was clearly species-specific, as demonstrated in the interaction of [CO_2] and SWC. Rising [CO_2] coupled with moistened soil generated increasing disparities of $\delta^{13}C$ between the water soluble compounds ($\delta^{13}C_{WSC}$) and estimated by gas-exchange observation ($\delta^{13}C_{obs}$) in *P. orientalis* with an amplitude of 0.0328‰–0.0472‰. Further, the differences between $\delta^{13}C_{WSC}$ and $\delta^{13}C_{obs}$ of *Q. variabilis* increased as CO_2 concentration increased and water stress alleviated (0.0384‰–0.0466‰). Fractionations from mesophyll conductance and post-photosynthesis both contributed to the total ^{13}C fractionation determined by two measurements (1.06%-24.94% and 75.30%-98.9% of total ^{13}C fractionation, respectively). Total ^{13}C fractionations were linearly dependent on g_s, indicating post-carboxylation fractionation was attributed to environmental variation. Thus, cautious descriptions of the magnitude and environmental dependence of apparent post-carboxylation fractionation are worth our attention in photosynthetic fractionation.

Key words: Post-carboxylation fractionation; Carbon isotope fractionation; Elevated CO_2 concentration; Soil volumetric water content; Instantaneous water use efficiency

1 Introduction

Since the onset of the industrial revolution, the atmospheric CO_2 concentration has increased at an annual rate of 0.4%, and is expected to increase further to 700 $\mu mol \cdot mol^{-1}$, together with more frequent periods of low water availability (IPCC, 2014). Increasing atmospheric CO_2 concentrations that trigger an ongoing greenhouse effect will not only lead to fluctuations in global patterns of precipitation, but also will amplify drought in arid regions, and lead to more frequent occurrences of extreme drought events (Lobell et al., 2014). Accompanying the increasing concentration of CO_2, the mean $\delta^{13}C$ of atmospheric CO_2 is depleted by 0.02‰–0.03‰ $year^{-1}$ (data available from the CU-INSTAAR/NOAACMDL network for atmospheric CO_2; http://www.esrl.noaa.gov/gmd/).

The carbon isotopic composition determined recently could respond more subtly to environmental changes and their influences on diffusion via plant physiology and metabolic processes (Gessler et al., 2014; Streit et al., 2013). While the depletion of $\delta^{13}C_{CO_2}$ has been shown in the atmosphere, variations in CO_2 concentration itself also might affect the $\delta^{13}C$ of plant organs that, in turn, respond physiologically to climatic change (Gessler et al., 2014). The carbon discrimination ($^{13}\Delta$) of leaves could also provide timely feedback about the availability of soil moisture and the atmospheric vapor pressure deficit (Cernusak et al., 2012). Discrimination against ^{13}C in leaves relies mainly on environmental factors that affect the ratio of intercellular to ambient CO_2 concentration (C_i/C_a) and Rubisco activities, even the mesophyll conductance derived from the difference of CO_2 concentrations between intercellular site and chloroplast (Farquhar et al., 1982; Cano et al., 2014). As changes in environmental conditions affect photosynthetic discrimination, they are expected to be recorded differentially in the $\delta^{13}C$ of water-soluble organic matter ($\delta^{13}C_{WSOM}$) of the different plant organs. Meanwhile, several processes during photosynthesis alter the $\delta^{13}C$ of carbon transported within plants considerably. Carbon-fractionation during photosynthetic CO_2 fixation has been described and reviewed well elsewhere (Farquhar et al., 1982; Farquhar and Sharkey, 1982).

Post-photosynthetic fractionation is derived from equilibrium and kinetic isotopic effects, which determines isotopic differences between metabolites and intramolecular reaction positions, defined as "post-photosynthetic" or "post-carboxylation" fractionation (Jäggi et al., 2002; Badeck et al., 2005; Gessler et al., 2008). Post-carboxylation fractionation in plants includes the carbon discriminations that follow carboxylation of ribulose-1, 5-bisphosphate, and internal diffusion (RuBP, 27‰), as well as related transitory starch metabolism (Gessler et al., 2008; Gessler et al., 2014), fractionation in leaves, fractionation-associated phloem transport, the remobilization or storage of soluble carbohydrates, and starch metabolism fractionations in sink tissue (tree rings). In the synthesis of soluble sugars, ^{13}C-depletions of triose phosphates occur during exportation from the cytoplasm, and during production of fructose-1, as does 6-bisphosphate by aldolase in transitory starch synthesis (Rossmann et al., 1991; Gleixner and Schmidt, 1997). Synthesis of sugars before transportation to the twig is associated with the post-carboxylation fractionation generated in leaves. Although these are likely to play a role, what should be also considered is the CO_2 concentration in the chloroplast (C_c), not in the intercellular space, as used in the simplified equation of the Farquar's model (Evans et al., 1986; Farquhar et al., 1989) is actually defined as carbon isotope discrimination ($\delta^{13}C$). Indeed, the difference between gas-exchange derived values and online measurements of $\delta^{13}C$ has been widely used to estimate C_i-C_c and mesophyll conductance for CO_2 (Le Roux et al., 2001; Warren and Adams, 2006; Flexas et al., 2006; Evans et al., 2009; Flexas et al., 2012; Evans and von Caemmerer 2013). In this regard, changes in mesophyll conductance could be partly responsible for the differences from two measurements, as it generally

82   increases in the short term in response to elevated CO_2 (Flexas et al., 2014), whereas it tends to decrease

83   under drought (Hommel et al., 2014; Théroux-Rancourt et al., 2014). Therefore, it is necessary to avoid

84   confusion of carbon isotope discrimination derived from synthesis of soluble sugars or/and mesophyll

85   conductance, and further, whether and what magnitude of these carbon fractionations are related to

86   environmental variation have not yet been investigated.

87   The simultaneous isotopic analysis of leaves is a recent refinement in isotope studies that allows us to

88   determine the temporal variation in isotopic fractionation (Rinne et al., 2016), and will help decipher

89   environmental conditions more reliably. Newly assimilated carbohydrates can be extracted, and are

90   defined as the water-soluble compounds (WSCs) in leaves (Brandes et al., 2006; Gessler et al., 2009),

91   which also can be associated with an assimilation-weighted average of C_i/C_a (and C_c/C_a)

92   photosynthesized over a period ranging from a few hours to 1-2 d (Pons et al., 2009). However, there is

93   dispute whether the fractionation stemmed from post-carboxylation or/and mesophyll resistance may

94   alter the stable signatures of leaf carbon and thence influence instantaneous water use efficiency (iWUE).

95   In addition, the way in which the iWUE derived from theses isotopic fractionations responds to different

96   environmental factors, such as elevated [CO_2] and/or soil water gradients, have not yet been observed.

97   Consequently, we investigated the $\delta^{13}C$ of the fast-turnover carbohydrate pool in leaves from saplings

98   of two trees typical in semi-arid areas of China—*Platycladus orientalis* and *Quercus variabilis*—together

99   with simultaneous gas exchange measurements in control-environment of growth chambers (FH-230).

100   Our goals are to differentiate the ^{13}C fractionation from the site of carboxylation to cytoplasm before

101   sugars transportation (total ^{13}C fractionation) of *P. orientalis* and *Q. variabilis*, which were determined

102   from the $\delta^{13}C$ of water-soluble compounds and gas-exchange measurements, and then to discuss the

103   potential causes for the observed divergence, estimate the contributions of post-photosynthetic and

104   mesophyll resistance on these differences, and describe how these carbon isotopic fractionations respond

105   to the interactive effects of elevated [CO_2] and water stress.

106   **2 Material and Methods**

107   **2.1 Study site and design**

108   Saplings of *P. orientalis* and *Quercus variabilis* were selected as experimental material from the

109   Capital Circle forest ecosystem station, a part of the Chinese Forest Ecosystem Research Network

110   (CFERN, 40°03'45"N, 116°5'45"E) in Beijing, China. This region is populated by warm, temperate,

111   deciduous, broad-leaved trees and mixed tree communities dominated by *Quercus variabilis* Bl. and

112   *Platycladus orientalis* (L.) Franco, respectively. Saplings have similar ground diameters, heights, and

113   growth statuses. The saplings were placed in pots 22 cm in diameter and 22 cm in height. Undisturbed

114   soil samples were collected from the field in the research region, and the sieved soil (with all particles

115   <10 mm removed) was placed in the pots. A single *P. orientalis* sapling was transplanted into each pot.

116   The soil bulk density in the pots was maintained at 1.337–1.447 g cm^{-3}. After one month of rejuvenation,

117   the potted saplings were placed into chambers for cultivation.

118   The controlled experimental treatments were conducted in growth chambers (FH-230, Taiwan Hipoint

119   Corporation, Kaohsiung City, Taiwan). To imitate the meteorological factors of the growth seasons in

120   the research region, the daytime temperature in the chambers was set to 25 ±0.5℃ from 07:00 to 17:00,

121   and the night-time temperature was 18 ±0.5℃ from 17:00 to 07:00. Relative humidity was maintained

122   at 60% and 80% during the day and night, respectively. The light system was activated in the daytime

123   and shut down at night. The average daytime light intensity was maintained at 200–240 μmol m^{-2} s^{-1}.

124   CO_2 concentration was controlled by the central controlling system of the chambers (FH-230). Two
125   growth chambers (A and B) were used in our study. Chamber A was switched in turn to maintain a CO_2
126   concentration of 400 ± 50 ppm (during June 2–9, June 12–19, June 21–28, and July 2–9, 2015) and 500
127   ± 50 ppm (during July 11–18, July 22–29, August 4–11, and August 15–22, 2015). The other was
128   adjusted to maintain the CO_2 concentration at 600 ± 50 ppm (during June 2–9, June 12–19, June 21–28,
129   and July 2–9, 2015) and 800 ± 50 ppm (during July 11–18, July 22–29, August 4–11, and August 15–22,
130   2015). The CO_2 concentration in the chambers was set to maintain one target level (permitting a standard
131   deviation of ± 50 ppm) during cultivation. Thus, we employed a gradient of four CO_2 concentrations in
132   our study (400 ± 50 ppm, 500 ± 50 ppm, 600 ± 50 ppm, and 800 ± 50 ppm). Detectors inside the chambers
133   monitored and maintained the CO_2 concentrations continuously at the constant setting.

134   We designed a device to water the potted plants automatically to avoid heterogeneity caused by
135   interruptions in the watering process (Fig. 1). It consisted of the water storage tank, holder, controller,
136   soil moisture sensors, and drip irrigation components. Prior to use, the water tank was filled with water,
137   and the soil moisture sensor was inserted to a uniform depth in the soil. After connecting the controller
138   to an AC power supply, specific soil water could be set. The soil volumetric water content (SWC) of the
139   pot soil was monitored by the soil moisture sensors. Through the sensors, the chamber could determine
140   whether to water or stop watering the plants. Two drip irrigation devices were installed in both chambers,
141   respectively. After measuring the average Field Capacity (FC) of the pot soil (30.70%), five levels of
142   SWC were maintained before the orthogonal tests, as follows: 100% FC (or CK) (SWC approximately
143   27.63%–30.70%), 70%–80% of FC (SWC approximately 21.49%–24.56%), 60%–70% of FC (SWC
144   approximately 18.42%–21.49%), 50%–60% of FC (SWC approximately 15.35%–18.42%), and 35%–
145   45% of FC (SWC approximately 10.74%–13.81%). Each level of soil water was kept within the specific
146   range thereafter by the irrigation device.

147   After establishing the equilibrium circumstances of elevated CO_2 across the soil water gradients, the
148   saplings were ready for investigation. Each orthogonal treatment included three replicates, and each
149   replicate continued for 7 days. Pots were rearranged periodically to minimize non-uniform illumination.

150   Orthogonal tests: elevated CO_2 concentration gradient presented as 400 ppm, 500 ppm, 600 ppm, and
151   800 ppm, combined with a soil-water gradient 35%–45% of FC, 50%–60% of FC, 60%–70% of FC, and
152   70%–80% of FC and 100% FC (CK).

2.2 Foliar gas exchange measurement

154   Fully expanded primary annual leaves of the saplings were measured with a portable infrared gas
155   photosynthesis system (LI-6400, Li-Cor, Lincoln, US) before and after the 7-day cultivation in the
156   chambers. Four replicates were measured with each leaf and four leaves were chosen per tree in the gas-
157   exchange measurement. There were two saplings ready for one orthogonal treatment ($[CO_2] \times$ water
158   stress). The main photosynthetic parameters, such as net photosynthetic rate (P_n) and transpiration rate
159   (T_r), were measured. Based on the theories proposed by Von Caemmerer and Farquhar (1981), stomatal
160   conductance (g_s) and intercellular CO_2 concentration (C_i) were calculated by the Li-Cor software. Each
161   leaf was measured three times. Three leaves from each sapling were chosen, and three saplings were
162   measured within one orthogonal treatment. Instantaneous water use efficiency via gas exchange (WUE_{ge})
163   was calculated as the ratio of P_n to E.

2.3 Plant material collection and leaf water soluble compounds extraction

165   After gas exchange measurements, recently-expanded, eight sun leaves were removed per tree of two
166   species and two cultivated saplings per specie were replicated per treatment, and then were frozen

4

immediately in liquid nitrogen. A protocol adapted from Gessler et al. (2004) was used to extract the water-soluble compounds (WSCs). All samples were ground to fine powders using mortars and liquid nitrogen. 50 mg of ground leaves and 100 mg PVPP (polyvinylpolypyrrolidone) were weighed, mixed evenly, and incubated in 1mL double demineralized water for 60 min at 5℃ in a centrifuge tube. Then, the tubes were heated in 100℃ water for 3 min. After they cooled to room temperature, the supernatant was centrifuged at 12000 xg for 5 min and transferred 10 μL supernatant into tin capsule to be dried at 70℃. Folded capsules were then ready for $\delta^{13}C$ analysis of WSOM.

The samples of WSCs from leaves were combusted in an elemental analyzer (EuroEA, HEKAtech GmbH, Wegberg, Germany) and analyzed in the mass spectrometer (DELTA^{plus}XP, ThernoFinnigan). Carbon isotope signatures are expressed in δ-notation in parts per thousand, relative to the international Pee Dee Belemnite (PDB):

$$\delta^{13}C = \left(\frac{R_{sample}}{R_{standard}} - 1\right) \times 1000 \tag{1}$$

where $\delta^{13}C$ is the heavy isotope and R_{sample} and $R_{standard}$ refer to the isotope ratio between the particular substance and the corresponding standard, respectively. The precision of the repeated measurements was 0.1 ‰.

2.4 Isotopic calculation

2.4.1 ^{13}C fractionation from the site of carboxylation to cytoplasm before sugars transportation

Based on the linear model developed by Farquhar and Sharkey (1982), the isotope discrimination factor, Δ, was calculated as:

$$\Delta = \left(^{13}C_a - {}^{13}C_P\right)/\left(1 + {}^{13}C_P\right) \tag{2}$$

where $^{13}C_a$ is the isotope signature of ambient [CO$_2$] in the chamber; $^{13}C_P$ is the $^{13}C : {}^{12}C$ of the water-soluble compounds extracted from foliage. The $C_i{:}C_a$ is determined by:

$$C_i{:}C_a = (\Delta - a)/(b - a) \tag{3}$$

where C_i is the intercellular CO$_2$ concentration, and C_a is the ambient CO$_2$ concentration in the chamber; a is the discrimination dependent on a fraction factor (4‰). b is the discrimination during CO$_2$ fixation by ribulose 1,5- bisphosphate carboxylase/oxygenase (Rubisco) and internal diffusion (30‰). Instantaneous water use efficiency by gas-exchange measurements (WUE$_{ge}$) is calculated as:

$$WUE_{ge} = P_n{:}T_r = (C_a - C_i)/1.6\Delta e \tag{4}$$

where P_n is the net carbon assimilation, T_r is the molar rate of transpiration, and 1.6 is the diffusion ratio of stomatal conductance to water vapor to CO$_2$ in the chamber. Δe is the difference in water vapor pressure between the intracellular in leaves and ambient air, which may be calculated as:

$$\Delta e = e_{lf} - e_{atm} = 0.611 \times e^{17.502T/(240.97+T)} \times (1 - RH) \tag{5}$$

where e_{lf} and e_{atm} represent the extra- and intra-cellular water vapor pressure, respectively. T and RH is temperature and relative humidity on leaf surface. The instantaneous water use efficiency could be determined by the δ^{13}C$_{WSC}$ of leaves of two species, defined as WUE$_{cp}$:

$$WUE_{cp} = \frac{P_n}{T_r} = (1 - \varphi)\,(C_a - C_i)/1.6\Delta e = C_a(1 - \varphi)\left[\frac{b - \delta^{13}C_a + (b+1)\delta^{13}C_{WSC}}{(b-a)(1+\delta^{13}C_{WSC})}\right]/1.6\Delta e \tag{6}$$

φ is the ratio between carbohydrates consumed during respiration of the leaves and that of other organs at night (0.3). $\delta^{13}C_{WSC}$ is the carbon isotopic composition of water soluble compounds extracted from leaves.

206 Then the ^{13}C fractionation from the site of carboxylation to cytoplasm before sugars transportation (total

207 ^{13}C fractionation) can be estimated by the observed δ^{13}C of water soluble compounds from leaves

208 ($\delta^{13}C_{WSC}$) and the modeled δ^{13}C calculated from gas-exchange ($\delta^{13}C_{model}$). The $\delta^{13}C_{model}$ can be calculated

209 from Δ_{model} from Eqn. (2). The Δ_{model} can be determined by Eqns. (3 and 4) as:

210 $$\Delta_{model} = (b - a)\left(1 - \frac{1.6\Delta e WUE_{ge}}{C_a}\right) + a \tag{7}$$

211 $$\delta^{13}C_{model} = \frac{C_a - \Delta_{model}}{1 + \Delta_{model}} \tag{8}$$

212 $$\text{Total } ^{13}C \text{ fractionation} = \delta^{13}C_{WSC} - \delta^{13}C_{model} \tag{9}$$

213 2.4.2 Methodology of calculating mesophyll conductance

214 Actually, the carbon isotope discrimination is generated from the relative contribution of diffusion and

215 carboxylation, reflected by the ratio of CO_2 concentration at the site of carboxylation (C_c) to that in the

216 ambient environment surrounding plants (C_a). The carbon isotopic discrimination (Δ) could be presented

217 as (Farquhar et al. 1982):

218 $$\Delta = a_b \frac{C_a - C_s}{C_a} + a \frac{C_s - C_i}{C_a} + (e_s + a_l)\frac{C_i - C_c}{C_a} + b\frac{C_c}{C_a} - \frac{\frac{eR_D}{k} + f\Gamma_*}{C_a} \tag{10}$$

219 where $C_a, C_s, C_i,$ and C_c indicate the CO_2 concentrations in the ambient environment, at the boundary

220 layer of leaf, in the intercellular air spaces before entrancing into solution, and at the sites of

221 carboxylation, respectively; a_b is the fractionation for the CO_2 diffusion at the boundary layer (2.9‰);

222 a is the fractionation occurring CO_2 diffusion in still air (4‰); e_s is the discrimination of CO_2 diffusion

223 when CO_2 enters in solution (1.1‰, at 25 ℃); a_l is the fractionation derived from diffusion in the

224 liquid phase (0.7‰); b is the carboxylation discrimination in C3 plants (27‰); e and f are carbon

225 discrimination derived in dark respiration (R_D) and photorespiration, respectively. k is the carboxylation

226 efficiency, and Γ^* is the CO_2 compensation point in the absence of dark respiration (Brooks and

227 Farquhar,1985).

228 When the gas in the cuvette could be well stirred during measurements of carbon isotopic discrimination

229 and gas exchange, the diffusion in the boundary layer could be neglected and Equation 7 could be shown:

230 $$\Delta = a\frac{C_a - C_i}{C_a} + (e_s + a_l)\frac{C_i - C_c}{C_a} + b\frac{C_c}{C_a} - \frac{\frac{eR_D}{k} + f\Gamma_*}{C_a} \tag{11}$$

231 There is no agreement about the value of e, although recent measurements estimated it as 0-4‰. Value

232 of f has been estimated ranging at 8-12‰ (Gillon and Griffiths, 1997; Igamberdiev et al., 2004;

233 Lanigan et al., 2008). As the most direct factor, the value of b will influence the calculation for g_m, has

234 been thought to be close to 30‰ in higher plants (Guy et al., 1993).

235 The difference of CO_2 concentration between the substomatal cavities and the chloroplast is omitted

236 while diffusion discrimination related with dark-respiration and photorespiration is also negligible, the

237 Equation 8 could be simplified as:

238 $$\Delta_i = a + (b - a)\frac{C_i}{C_a} \tag{12}$$

239 Equation 12 presents the linear relationship between carbon discrimination and C_i/C_a that used

240 normally in carbon isotopic fractionation. That underlined the subsequent comparison between the

241 expected Δ (originated from gas-exchange, Δ_i) and those actually measured (Δ_{obs}), which could

242 evaluate the magnitude of differences of CO_2 concentration between the intercellular air and the sites of

243 carboxylation that generated by mesophyll resistance. Consequently, g_m can be estimated by

244 performing the Δ_{obs} by isotope ratio mass spectrometry and expected Δ_i from C_i/C_a by gas exchange

245 measurements.

246 Then subtract Δ_{obs} of Equation 11 from Δ_i calculated by Equation 12:

247 $$\Delta_i - \Delta_{obs} = (b - e_s - a_l)\frac{C_i - C_c}{C_a} + \frac{\frac{eR_D}{k} + f\Gamma^*}{C_a} \qquad (13)$$

248 and the net assimilation rate (A_n) from the first Fick's law is presented by:

249 $$A_n = g_m(C_i - C_c) \qquad (14)$$

250 Substitute Equation 14 into Equation 13 we obtain:

251 $$\Delta_i - \Delta_{obs} = (b - e_s - a_l)\frac{A_n}{g_m C_a} + \frac{\frac{eR_D}{k} + f\Gamma^*}{C_a} \qquad (15)$$

252 $$g_m = \frac{(b - e_s - a_l)\frac{A_n}{C_a}}{(\Delta_i - \Delta_{obs}) - \frac{eR_D/k + f\Gamma^*}{C_a}} \qquad (16)$$

253 In calculation of g_m, the respiratory and photorespiratory terms could be ignored or be given the

254 specific constant values. Here, e and f are assumed to be zero or be cancelled out in the calculation of

255 g_m.

256 Then Equation 16 can be transformed into:

257 $$g_m = \frac{(b - e_s - a_l)\frac{A_n}{C_a}}{\Delta_i - \Delta_{obs}} \qquad (17)$$

258 **3 Results**

259 **3.1 Foliar gas exchange measurements**

260   *P. orientalis* and *Q. variabilis* saplings were exposed to the orthogonal treatments (under gradients of

261 SWC and [CO_2] of 400 ppm, 500 ppm, 600 ppm, and 800 ppm, labeled as C_{400}, C_{500}, C_{600}, and C_{800}).

262 When SWC increased, P_n, g_s and T_r in *P. orientalis* and *Q. variabilis* peaked at 70%−80% of FC or/and

263 FC (Fig. 2). The C_i in *P. orientalis* rose as SWC increased, while it peaked at 60%−70% of FC and

264 declined thereafter with increased SWC in *Q. variabilis*. The uptake capacity of carbon and C_i were

265 elevated significantly by elevated [CO_2] at any given SWC for two species ($p<0.05$). Further, greater

266 increasing magnitudes of P_n in *P. orientalis* were found at 50%−70% of FC from C_{400} to C_{800}, which was

267 at 35%−45% of FC in *Q. variabilis*. As the water stress was alleviated (at 70%−80% of FC and FC), the

268 reduction of g_s in *P. orientalis* was more pronounced with elevated [CO_2] at a given SWC ($p<0.01$).

269 Nevertheless, g_s of *Q. variabilis* in C_{400}, $C_{500,}$ and C_{600} was significantly higher than that in C_{800} at 50%−

270 80% of FC ($p<0.01$). Coordinated with g_s, T_r of two species in C_{400} and C_{500} was significantly higher than

271 that in C_{600} and C_{800} except for 35%−60% of FC ($p<0.01$, Figs. 2g and 2h). Larger P_n, g_s, C_i and T_r of *Q.*

272 *variabilis* was significantly presented than that of *P. orientalis* ($p<0.01$, Fig. 2).

273 **3.2 $\delta^{13}C$ of water-soluble compounds in leaves**

274   To observe the photosynthetic traits of the two saplings, the same leaf was frozen immediately and the

275 water-soluble compounds (WSCs) were extracted for all orthogonal treatments. $\delta^{13}C_{WSC}$ ($\delta^{13}C$ of water-

276 soluble compounds from leaves) of two species both increased as soil moisture improved (Figs. 3a and

277 3b, $p<0.01$). The average ($\pm$SD) $\delta^{13}C_{WSC}$ of *P. orientalis* and *Q. variabilis* ranged from -27.44 $\pm0.155‰$

278 to -26.71 $\pm0.133‰$, and from -27.96 $\pm0.129‰$ to -26.49 $\pm0.236‰$, respectively. Similarly with the

279 photosynthetic capacity varying with increased SWC, average $\delta^{13}C_{WSC}$ of two saplings reached their

280 maximums at 70%−80% of FC. Together with the gradual enrichment of [CO_2], average $\delta^{13}C_{WSC}$ in two

281 species declined while [CO_2] exceeded 600 ppm ($p<0.01$). Except for C_{400} at 50%−100% of FC, $\delta^{13}C_{WSC}$

282 of *P. orientalis* was significantly larger than that of *Q. variabilis* in any [CO_2] $\times$ SWC treatment ($p<0.01$,

283   Fig. 3).

3.3 Estimations of WUE_{ge} and WUE_{cp}

    Instantaneous water use efficiency via gas exchange (WUE_{ge}) is calculated as P_n divided by T_r. Figure 4a shows that incremental magnitudes of WUE_{ge} in *P. orientalis* under severe drought (i.e., 35%−45% of FC) were highest at any given $[CO_2]$, ranging from 90.70% to 564.65%. WUE_{ge} in *P. orientalis* reduced as SWC increased, while they increased remarkably as $[CO_2]$ elevated. Compared to *P. orientalis*, trends of WUE_{ge} in *Q. variabilis* were promoted slightly at FC in C_{600} or C_{800} as soil moistened (Fig. 4b). The maximum of WUE_{ge} thus occurred at 35%−45% of FC in C_{800} among all orthogonal treatments for *P. orientalis*, as well as that for *Q. variabilis*. Further, elevated $[CO_2]$ enhanced the WUE_{ge} of *Q. variabilis* clearly at any SWC except that at 60%−80% of FC. Most saplings of *P. orientalis* had greater WUE_{ge} than did *Q. variabilis* between the same $[CO_2] \times SWC$ treatments ($p<0.05$).

    The instantaneous water use efficiency could be determined from Eqn. (6) by the $\delta^{13}C_{WSC}$ of leaves of two species, defined as WUE_{cp}. As illustrated in Fig. 5a, WUE_{cp} of *P. orientalis* in C_{600} or C_{800} climbed up as water stress alleviated beyond 50%−60% of FC, while the water threshold was 60%−70% of FC in C_{400} or C_{500}. *Q. variabilis* exhibited no uniform trend of WUE_{cp} with soil wetting (Fig. 5b). Except for C_{400}, WUE_{cp} of *Q. variabilis* decreased abruptly at 50%−60% of FC, and then rose as soil moisture improved in C_{500}, C_{600}, and C_{800}. In contrast to the findings about WUE_{ge} in two species, WUE_{cp} of *Q. variabilis* was more pronounced than that of *P. orientalis* among all orthogonal treatments.

3.4 ^{13}C fractionation from the site of carboxylation to cytoplasm before sugars transportation

    We evaluated the total ^{13}C fractionation from the site of carboxylation to cytoplasm by gas exchange and δ^{13}C of water-soluble compounds from leaf measurements (Table 1), which can retrace ^{13}C fractionation before carboxylation transport to the twig. Comparing $\delta^{13}C_{WSC}$ with $\delta^{13}C_{model}$ from Eqns. (4, 7 and 8), total ^{13}C fractionation of *P. orientalis* ranged from 0.0328‰ to 0.0472‰, which was smaller than that of *Q. variabilis* (0.0384‰ to 0.0466‰). The total fractionations of *P. orientalis* were magnified with soil wetting especially that was increased by 21.30%−42.04% at 35%−80% of FC from C_{400} to C_{800}. Fractionation coefficients under C_{400} and C_{500} were amplified as SWC increased until 50%−60% of FC in *Q. variabilis*, whereas it was increased at 50%−80% of FC and decreased at FC under C_{600} and C_{800}. Elevated $[CO_2]$ enhanced the average fractionation effect of *P. orientalis*, while those of *Q. variabilis* declined sharply from C_{600} to C_{800}. Total ^{13}C fractionation in *P. orientalis* increased faster than did those of *Q. variabilis* with increased soil moisture.

3.5 g_m imposed on the interaction of CO_2 concentration and water stress

    According to comparison between online leaf $\delta^{13}C_{WSC}$ and the values of gas exchange measurements, g_m over all treatments was presented in Fig. 6 (Eqns. 10-17). Significant increment trend of g_m was observed with water stress alleviated in *P. orientalis*, ranging from 0.0091–0.0690 mol CO_2 m^{-2} s^{-1} ($p<0.05$), which reached the maximums at FC under a given $[CO_2]$. Yet increases in g_m of *Q. variabilis* with increasing SWC become unremarkable except that under C_{400}. With CO_2 concentration elevated, g_m of two species was increased in different degrees. Comparing with *P. orientalis* under C_{400}, g_m was increased gradually and reached its maximum under C_{800} at 35%−60% of FC and FC ($p<0.05$), however, that was maximized under C_{600} ($p<0.05$) and slipped down under C_{800} at 60%−80% of FC. The maximum increment magnitude of g_m (8.2%−58.4%) occurred at C_{800} at any given SWC in *Q. variabilis*. It is evidently shown that g_m of *Q. variabilis* was larger than that of *P. orientalis* in the same treatment.

3.6 The contribution of post-carboxylation fractionation

325   Here, the difference between Δ_i and Δ_{obs} presented the ^{13}C fractionation derived from mesophyll

326 conductance. So the post-photosynthetic fractionation after carboxylation can be calculated by

327 subtracting the fractionation derived from mesophyll conductance from the total ^{13}C fractionation that is

328 generated from the site of carboxylation to cytoplasm before sugars transportation (Table 1). The

329 fractionation from g_m had less contribution to total ^{13}C fractionation than that from synthesis of sugars

330 belong to post-carboxylation fractionation in any given treatment (Table 1). The contributions of

331 fractionation from g_m with two species were illustrated different variations with soil water increasing,

332 which declined at 50%−80% of FC and rose up at FC in *P. orientalis*, yet it was shown increasing with

333 water stress alleviated at 50%−80% of FC and then decreased at FC in *Q. variabilis*. Nevertheless, the

334 fractionations from synthesis of sugars in leaf and these contributions to total fractionation were all

335 increased as soil moistened with two species. Considering the effects of enriched $[CO_2]$ on fractionations

336 of mesophyll conductance, the fractionation from mesophyll conductance reached its average peak under

337 C_{600} in *P. orientalis*, which occurred under C_{800} with *Q. variabilis*. Post-photosynthetic fractionations

338 were increased along with $[CO_2]$ elevated in *P. orientalis*, which reached those maximums under C_{600}

339 and then slipped down differing in degrees under C_{800}.

340 **3.7 Relationship between g_s, g_m and total ^{13}C fractionation**

341   Stoma is the conduit between the plant and atmosphere. Total ^{13}C fractionation after carboxylation

342 may be correlated with resistances derived from stomata and mesophyll cells. Here, we performed linear

343 regressions between g_s/g_m and total ^{13}C fractionation coefficient for *P. orientalis* and *Q. variabilis*,

344 respectively (Fig. 7 and 8). It was apparent that total ^{13}C fractionation coefficient was linearly dependent

345 on the g_s ($p<0.05$), which controls the exchange of CO_2 and H_2O, and responds to environmental variation.

346 Subsequently, it was shown the linear relationships between g_m and the total ^{13}C fractionation coefficient,

347 reflecting variation of CO_2 concentration through the chloroplast was correlated with the carbon

348 discrimination happened after photosynthesis in the leaf.

349 **4 Discussion**

350 **4.1 Photosynthetic traits**

351   The exchange of CO_2 and water vapor via stomata is modulated in part by the soil or leaf water

352 potential (Robredo et al., 2010). Saplings of *P. orientalis* reached their maximums of P_n and g_s at 70%−

353 80% of FC under any $[CO_2]$. As SWC exceeded the water threshold, elevated CO_2 caused a greater

354 reduction in g_s, as has been reported for barley and wheat (Wall et al., 2011). Further, Maximal g_s of *Q.*

355 *variabilis* in C_{400}, C_{500}, C_{600}, and C_{800} were generated successively as soil moisture increased, indicating

356 that relative drought can stimulate the stomata which are more sensitive to environmental changes. In

357 addition, C_i of *Q. variabilis* peaked at 60%−70% of FC and followed declines as soil moisture increased

358 (Wall et al., 2006; Wall et al., 2011). This is interpreted as stomata having the tendency to maintain a

359 constant C_i or C_i/C_a when ambient $[CO_2]$ increases, which would determine the CO_2 used directly in

360 chloroplast (Yu et al., 2010). On the basis of theories (Farquhar and Sharkey, 1982) and common

361 experimental technologies (Xu, 1997), this could be explained as the stomatal limitation. However, C_i of

362 *P. orientalis* was increased considerably while SWC exceeded 70%−80% of FC, as found by Mielke et

363 al. (2000). One factor that can account for that is plants close their stomata to reduce intensive loss of

364 water during the synthesis of organic matter, simultaneously decreasing the availability of CO_2 and

365 generating respiration of organic matter (Robredo et al., 2007). Another explanation is the limited root

366 volume in potted experiments may not be able to absorb sufficient water to support full growth of shoots

9

367 (Leakey et al., 2009; Wall et al., 2011). In our study, further increasing [CO$_2$] may cause nonstomatal
368 limitation as SWC exceeding the threshold (70%−80% of FC), i.e., accumulation of nonstructural
369 carbohydrates in leaf tissue that induces mesophyll-based and/or biochemical-based transient inhibition
370 of photosynthetic capacity (Farquhar and Sharkey, 1982). Xu and Zhou (2011) developed a five-level
371 SWC gradient to examine the effect of water on the physiological characteristics of perennial *Leymus*
372 *chinensis*, demonstrating that there was the soil water irrigation maximum below which the plant could
373 manage itself to adjust changing environment. Miranda Apodaca et al. (2015) also concluded that, in
374 suitable water conditions, elevated CO$_2$ augmented CO$_2$ assimilation of herbaceous plants.

375 The P_n of the two species increased with elevated [CO$_2$] in our study, similarly with the results from
376 C$_3$ woody plants (Kgope et al., 2010). Further, increasing [CO$_2$] alleviated severe drought and heavy
377 irrigation, which verifies that photosynthetic inhibition produced by water stress or excess may be
378 mediated by increased [CO$_2$] (Robredo et al., 2007; Robredo et al., 2010) and meliorate the adverse
379 effects of drought stress by decreasing plant transpiration (Kirkham, 2016; Kadam et al., 2014; Miranda
380 Apodaca et al., 2015; Tausz Posch et al., 2013).

4.2 Differences between WUE$_{ge}$ and WUE$_{cp}$

382 The increments of WUE$_{ge}$ in *P. orientalis* and *Q. variabilis* that resulted from the combination of an
383 increase in P_n and decrease in g_s, followed by the reduction of T_r (Figs. 2a, 2g, 2b and 2h), also were
384 demonstrated by Ainsworth and McGrath (2010). Combining P_n and T_r of two species in the same
385 treatment, lower WUE$_{ge}$ in *Q. variabilis* is obtained due to its physiological and morphological traits,
386 such as larger leaf area, rapid growth, and higher stomatal conductance than that of *P. orientalis* (Adiredjo
387 et al., 2014). Medlyn et al. (2001) reported that the stomatal conductance of broadleaved species is more
388 sensitive to elevated CO$_2$ concentrations than is that of conifers. Moreover, there has been no consensus
389 on the patterns of iWUE with related soil water states at the leaf level, although some have discussed this
390 topic (Yang et al., 2010). The WUE$_{ge}$ of *P. orientalis* and *Q. variabilis* was enhanced with water drying,
391 as presented by Parker and Pallardy (1991), DeLucia and Heckathorn (1989), and Reich et al. (1989).
392 Leakey (2009) also concluded that the WUE of plants in drought could be increased substantially, which
393 was shown more clearly with elevated [CO$_2$] in this study.

394 Bögelein et al. (2012) confirmed that WUE$_{cp}$ was more consistent with daily mean WUE$_{ge}$ than was
395 WUE$_{phloem}$. The WUE$_{cp}$ of two species demonstrated similar variation to those of δ^{13}C$_{WSC}$, which
396 differentiated with that of WUE$_{ge}$. Pons et al. (2009) reviewed that $\varDelta$ in the leaf soluble sugar is coupled
397 tightly with dynamics in the environment integrated over a period ranging from a few hours to 1−2 d.
398 WUE$_{cp}$ of our materials responded synthetically with SWC × [CO$_2$] gradients over cultivated days
399 whereas WUE$_{ge}$ is characterized by the instantaneous state of plants to conditions. In addition, species-
400 specific δ^{13}C$_{WSC}$ were observed in the same condition. Consequently, WUE$_{cp}$ and WUE$_{ge}$ have different
401 variable curves according to treatments.

4.3 The influence of mesophyll conductance on the fractionation after carboxylation

403 The consensus has been reached that the routine of CO$_2$ diffusion into photosynthetic site in plant
404 includes two main procedures, which are CO$_2$ moving from ambient environment surrounding the leaf
405 (C_a) to the sub-stomatic cavities (C_i) through stomata, and from there to the site of carboxylation within
406 the chloroplast stroma (C_c) of leaf mesophyll. The latter diffusion is defined as mesophyll conductance
407 (g_m) (Flexas et al., 2008). Moreover, g_m has been identified to coordinate with environmental variables
408 at the faster rate than that of stomatal conductance (Galmés et al., 2007; Tazoe et al., 2011; Flexas et al.,
409 2007). During our 7-day cultivations of water stress × [CO$_2$], g_m increased and WUE$_{ge}$ was decreased as

soil moistened, which has been verified that g_m as the important factor could improve WUE under drought pretreatment (Han et al., 2016). There has been a dispute how g_m responds to fluctuation of CO_2 concentration. Terashima *et al.* (2006) have confirmed that CO_2 permeable aquaporin, located in the plasma membrane and inner envelope of chloroplasts (Uehlein et al. 2008), could regulate the change of g_m. In our study, different species has specific-special g_m responding to the gradient of [CO_2]. g_m of *P. orientalis* were significantly reduced by 9.08%-44.42% as [CO_2] rising from 600 to 800 ppm at 60%-80% of FC, being similar to the results obtained by Flexas *et al.* (2007). Although larger g_m of *Q. variabilis* under C_{800} was observed, it made almost no difference.

Furthermore, g_m contributed to the ^{13}C fractionation following the carboxylation while photosynthate has not been transported to the twigs of plant. The ^{13}C fractionation of CO_2 from air surrounding leaf to sub-stomatal cavity may be simply considered, whereas the fractionation induced by mesophyll conductance from sub-stomatic cavities to the site of carboxylation in the chloroplast cannot be neglected (Pons et al., 2009; Cano et al., 2014). As estimating the post-photosynthetic fractionation in leaf, carbon discrimination generated by mesophyll conductance must be subtracted from ^{13}C fractionation from the site of carboxylation to cytoplasm before sugars transportation (the difference between $\delta^{13}C_{WSC}$ and $\delta^{13}C_{model}$), which was closely associated with g_m (Fig 8, $p<0.05$). Similar variations of fractionation derived from g_m were presented with that of g_m under orthogonal tests on Table 1.

4.4 Post-carboxylation fractionation generated before photosynthate leaving leaves

Photosynthesis, a biochemical and physiological process (Badeck et al., 2005), is characterized by discrimination against ^{13}C, which leaves an isotopic signature in the photosynthetic apparatus. There is already a classic review of the carbon-fractionation in leaves (Farquhar et al., 1989) that covers the significant aspects of photosynthetic carbon isotope discrimination. The post-photosynthetic fractionation associated with the metabolic pathways of non-structural carbohydrates (NSC; defined here as soluble sugars + starch) within leaves, and fractionation during translocation, storage, and remobilization prior to tree ring formation remain unclear (Epron et al., 2012; Gessler et al., 2014; Rinne et al., 2016). The synthetic processes of sucrose and starch before transportation to the twig are within the domain of post-carboxylation fractionation generated in leaves. Hence, we hypothesized that ^{13}C fractionation might exist. When we finished the leaf gas exchange measurements, the leaf samples were collected immediately to determine the $\delta^{13}C$ of water-soluble compounds ($\delta^{13}C_{WSC}$). Presumably, the ^{13}C fractionation generated in the synthetic processes of sucrose and starch was approximately contained within the ^{13}C fractionation from the site of carboxylation to cytoplasm before sugars transportation as total ^{13}C fractionation. When comparing $\delta^{13}C_{WSC}$ with $\delta^{13}C_{obs}$, total fractionations of *P. orientalis* ranged from 0.0328‰ to 0.0472‰, less than that of *Q. variabilis* (from 0.0384‰ to 0.0466‰). Then total ^{13}C fractionation subtracted by fractionation derived from mesophyll conductance, post-photosynthetic fractionation occupied 75.30%-98.9% of total ^{13}C fractionation. Recently, Gessler et al. (2004) reviewed the environmental drivers of variation in photosynthetic carbon isotope discrimination in terrestrial plants. The ^{13}C fractionation of *P. orientalis* were enhanced by soil moistening, consistent with that of *Q. variabilis*, except at FC. The ^{13}C isotope signature of *P. orientalis* was dampened by elevated [CO_2]. Yet, ^{13}C-depletion was weakened in *Q. variabilis* in C_{600} and C_{800}. Linear regression between g_s and total ^{13}C fractionation coefficient indicated that the post-carboxylation fractionation in leaves depended on the variation of g_s and stomata aperture correlated with environmental change.

5 Conclusions

Through orthogonal treatments of four [CO_2] $\times$ five SWC, WUE_{cp} calculated by $\delta^{13}C$ of water-soluble compound and WUE_{ge} derived from simultaneous leaf gas exchange for leaves were estimated to differentiate the $\delta^{13}C$ signal variation before leaf-exported translocation of primary assimilates. The influence of mesophyll conductance on the difference of ^{13}C fractionation between the sub-stomatic cavities and the ambient environment need to be considered, while testing the hypothesis that the post-carboxylation will contribute to the ^{13}C fractionation from the site of carboxylation to cytoplasm before sugars transportation. In response to the interactive effects of [CO_2] and SWC, WUE_{ge} of the two species of saplings both decreased with soil moistening, and increased with elevated [CO_2] at 35%–80% of FC. We concluded that relative soil drying, coupled with elevated [CO_2], could improve WUE_{ge} by strengthening photosynthetic capacity and reducing transpiration. WUE_{ge} of *P. orientalis* was significantly greater than was that of *Q. variabilis*, while the opposite was the case for WUE_{cp} in two species. Mesophyll conductance and post-photosynthesis were manifested both contributing to the ^{13}C fractionation from the site of carboxylation to cytoplasm before sugars transportation determined by gas exchange and carbon isotopic measurements. Rising [CO_2] and/or soil moistening generated increasing disparities between $\delta^{13}C_{WSC}$ and $\delta^{13}C_{model}$ in *P. orientalis*; nevertheless, the differences between $\delta^{13}C_{WSC}$ and $\delta^{13}C_{model}$ in *Q. variabilis* increased as [CO_2] being less than 600 ppm and/or water stress was alleviated. Total ^{13}C fractionation in leaf was linearly dependent on g_s. With respect to carbon fractionation in post-carboxylation and transportation processes, we cannot neglect that the instantaneous water use efficiency derived from the synthesis of sucrose and starch were influenced inevitably by environmental changes. Thus, cautious descriptions of the magnitude and environmental dependence of apparent post-carboxylation fractionation are worth our attention in photosynthetic fractionation.

References

Adiredjo, A. L., Navaud, O., Lamaze, T., and Grieu, P.: Leaf carbon isotope discrimination as an accurate indicator of water use efficiency in sunflower genotypes subjected to five stable soil water contents, J Agron. Crop Sci., 200, 416–424, 2014.

Ainsworth, E. A. and McGrath, J. M.: Direct effects of rising atmospheric carbon dioxide and ozone on crop yields, Climate Change and Food Security, Springer, 109–130, 2010.

Badeck, F. W., Tcherkez, G., Eacute, N. S. S., Piel, C. E. M., and Ghashghaie, J.: Post-photosynthetic fractionation of stable carbon isotopes between plant organ – a widespread phenomenon, Rapid Commun. Mass S., 19, 1381–1391, 2005.

Bögelein, R., Hassdenteufel, M., Thomas, F. M., and Werner, W.: Comparison of leaf gas exchange and stable isotope signature of water-soluble compounds along canopy gradients of co-occurring Douglas-fir and European beech, Plant Cell Environ., 35, 1245–1257, 2012.

Brandes, E., Kodama, N., Whittaker, K., Weston, C., Rennenberg, H., Keitel, C., Adams, M. A., and Gessler, A.: Short-term variation in the isotopic composition of organic matter allocated from the leaves to the stem of *Pinus sylvestris*: effects of photosynthetic and postphotosynthetic carbon isotope fractionation, Global Change Biol., 12, 1922–1939, 2006.

Brooks, A. and Farquhar, G. D.: Effect of temperature on the CO_2/O_2 specificity of ribulose-1,5-bisphosphate carboxylase/oxygenase and the rate of respiration in the light, Planta, 165, 397–406, 1985.

Brugnoli E, Farquhar GD. 2000. Photosynthetic fractionation of carbon isotopes. In: Leegood RC, Sharkey TD, von Caemmerer S. eds. Photosynthesis: physiology and metabolism. Advances in photosynthesis. Dordrecht, The Netherlands: Kluwer Academic Publishers, 399–434.

Cano, F. J., López, R., and Warren, C. R.: Implications of the mesophyll conductance to CO_2 for photosynthesis and water-use efficiency during long-term water stress and recovery in two contrasting Eucalyptus species, Plant Cell Environ., 37, 2470–2490, 2014.

Cernusak, L. A., Ubierna, N., Winter, K., Holtum, J. A. M., Marshall, J. D., and Farquhar, G. D.: Environmental and physiological determinants of carbon isotope discrimination in terrestrial plants, New Phytologist, 200, 950–965, 2013.

DeLucia, E. H. and Heckathorn, S. A.: The effect of soil drought on water-use efficiency in a contrasting Great Basin desert and Sierran montane species, Plant Cell Environ., 12, 935–940, 1989.

Epron, D., Nouvellon, Y., and Ryan, M. G.: Introduction to the invited issue on carbon allocation of trees and forests, Tree physiol., 32, 639–643, 2012.

Evans, J. R., Kaldenhoff, R., Genty, B., and Terashima, I.: Resistances along the CO_2 diffusion pathway inside leaves, J. Exp. Bot., 60, 2235–2248, 2009.

Evans, J. R., Sharkey, T. D., Berry, J. A., and Farquhar, G. D.: Carbon isotope discrimination measured concurrently with gas-exchange to investigate CO_2 diffusion in leaves of higher-plants, Funct. Plant Biol., 13, 281–292, 1986.

Evans, J. R. and von Caemmerer, S.: Temperature response of carbon isotope discrimination and mesophyll conductance in tobacco, Plant Cell Environ., 36, 745–756, 2013.

Farquhar, G. D., Ehleringer, J. R., and Hubick, K. T.: Carbon isotope discrimination and photosynthesis, Ann. Rev. Plant Physiol., 40, 503–537, 1989.

Farquhar, G. D., O'Leary, M. H., and Berry, J. A.: On the relationship between carbon isotope discrimination and the intercellular carbon dioxide concentration in leaves, Funct. Plant Biol., 9, 121–137, 1982.

Farquhar, G. D. and Sharkey, T. D.: Stomatal conductance and photosynthesis, Ann. Rev. Plant Physiol., 33, 317–345, 1982.

Flexas, J., Barbour, M. M., Brendel, O., Cabrera, H. M., Carriquí M., Díaz-Espejo, A., Douthe, C., Dreyer, E., Ferrio, J. P., Gago, J., Gallé, A., Galmés, J., Kodama, N., Medrano, H., Niinemets, Ü., Peguero-Pina, J. J., Pou, A., Ribas-Carbó, M., Tomás, M., Tosens, T., and Warren, C. R.: Mesophyll diffusion conductance to CO_2: An unappreciated central player in photosynthesis, Plant Science, 193–194, 70–84, 2012.

Flexas, J., Carriquí M., Coopman, R. E., Gago, J., Galmés, J., Martorell, S., Morales, F., and Diaz-Espejo, A.: Stomatal and mesophyll conductances to CO_2 in different plant groups: Underrated factors for predicting leaf photosynthesis responses to climate change? Plant Science, 226, 41–48, 2014.

Flexas, J., Diaz-Espejo, A., Galmés, J., Kaldenhoff, R., Medano, H., and Ribas-Carbo, M.: Rapid variations of mesophyll conductance in response to changes in CO_2 concentration around leaves, Plant Cell Environ., 30, 1284–1298, 2007.

Flexas, J., Ribas-Carbó, M., Diaz-Espejo, A., Galmés, J., and Medrano, H.: Mesophyll conductance to CO_2: current knowledge and future prospects, Plant Cell Environ., 31, 602–621, 2008.

Flexas, J., Ribas-Carbó, M., Hanson, D.T., Bota, J., Otto, B., Cifre, J., McDowell, N., Medrano, H., and Kaldenhoff, R.: Tobacco aquaporin NtAQP1 is involved in mesophyll conductance to CO_2 *in vivo*, Plant J., 48, 427–439, 2006.

Galmés, J., Medrano, H., and Flexas, J.: Photosynthetic limitations in response to water stress and recovery in Mediterranean plants with different growth forms, New Phytol., 175, 81–93. 2007.

Gessler, A., Brandes, E., Buchmann, N., Helle, G., Rennenberg, H., and Barnard, R. L.: Tracing carbon

539   and oxygen isotope signals from newly assimilated sugars in the leaves to the tree-ring archive,

540   Plant Cell Environ., 32, 780–795, 2009.

541   Gessler, A., Ferrio, J. P., Hommel, R., Treydte, K., Werner, R. A., and Monson, R. K.: Stable isotopes

542   in tree rings: towards a mechanistic understanding of isotope fractionation and mixing processes

543   from the leaves to the wood, Tree Physiol., 34, 796–818, 2014.

544   Gessler, A., Rennenberg, H., and Keitel, C.: Stable isotope composition of organic compounds

545   transported in the phloem of European beech-evaluation of different methods of phloem sap

546   collection and assessment of gradients in carbon isotope composition during leaf-to-stem transport,

547   Plant Biology, 6, 721–729, 2004.

548   Gessler, A., Tcherkez, G., Peuke, A. D., Ghashghaie, J., and Farquhar, G. D.: Experimental evidence for

549   diel variations of the carbon isotope composition in leaf, stem and phloem sap organic matter in

550   *Ricinus communis*, Plant Cell Environ., 31, 941–953, 2008.

551   Gillon, J. S., Griffiths, H.: The influence of (photo)respiration on carbon isotope discrimination in plants.

552   Plant Cell Environ., 20, 1217–1230, 1997.

553   Gleixner, G. and Schmidt, H.: Carbon isotope effects on the fructose-1, 6-bisphosphate aldolase reaction,

554   origin for non-statistical ^{13}C distributions in carbohydrates, J. Biol. Chem., 272, 5382–5387, 1997.

555   Guy, R. D., Fogel, M. L., and Berry, J. A.: Photosynthetic fractionation of the stable isotopes of oxygen

556   and carbon, Plant Physiol., 101, 37–47, 1993.

557   Han, J. M., Meng, H. F., Wang, S. Y., Jiang, C. D., Liu, F., Zhang, W. F., and Zhang, Y. L.: Variability

558   of mesophyll conductance and its relationship with water use efficiency in cotton leaves under

559   drought pretreatment, J. Plant Physiol., 194, 61–71, 2016.

560   Hommel, R., Siegwolf, R., Saurer, M., Farquhar, G. D., Kayler, Z., Ferrio, J. P., and Gessler, A.: Drought

561   response of mesophyll conductance in forest understory species-impacts on water-use efficiency

562   and interactions with leaf water movement, Physiol. Plantarum, 152, 98–114, 2014.

563   Igamberdiev, A. U., Mikkelsen, T. N., Ambus, P., Bauwe, H., and Lea, P. J.: Photorespiration contributes

564   to stomatal regulation and carbon isotope fractionation: a study with barley, potato and Arabidopsis

565   plants deficient in glycine decarboxylase, Photosynth. Res., 81, 139–152, 2004.

566   IPCC: Summary for policymakers, in: Climate Change 2014, Mitigation of Climate Change, contribution

567   of Working Group III to the Fifth Assessment Report of the Intergovernmental Panel on Climate

568   Change, edited by: Edenhofer, O., Pichs-Madruga, R., Sokona, Y., Farahani, E., Kadner, S., Seyboth,

569   K., Adler, A., Baum, I., Brunner, S., Eickemeier, P., Kriemann, B., Savolainen, J., Schlomer, S.,

570   von Stechow, C., Zwickel, T., and Minx, J. C., Cambridge University Press, Cambridge, UK and

571   New York, NY, USA, 1–30, 2014.

572   Jäggi, M., Saurer, M., Fuhrer, J., and Siegwolf, R.: The relationship between the stable carbon isotope

573   composition of needle bulk material, starch, and tree rings in *Picea abies*, Oecologia, 131, 325–332,

574   2002.

575   Kadam, N. N., Xiao, G., Melgar, R. J., Bahuguna, R. N., Quinones, C., Tamilselvan, A., Prasad, P. V.

576   V., and Jagadish, K. S. V.: Chapter three-agronomic and physiological responses to high

577   temperature, drought, and elevated CO_2 interactions in cereals, Adv. Agron., 127, 111–156, 2014.

578   Kgope, B. S., Bond, W. J., and Midgley, G. F.: Growth responses of African savanna trees implicate

579   atmospheric [CO_2] as a driver of past and current changes in savanna tree cover, Austral Ecol., 35,

580   451–463, 2010.

581   Kirkham, M. B.: Elevated carbon dioxide: impacts on soil and plant water relations, CRC Press, London,

582   New York, 2016.

Kodama, N., Barnard, R. L., Salmon, Y., Weston, C., Ferrio, J. P., Holst, J., Werner, R. A., Saurer, M., Rennenberg, H., and Buchmann, N.: Temporal dynamics of the carbon isotope composition in a *Pinus sylvestris* stand: from newly assimilated organic carbon to respired carbon dioxide, Oecologia, 156, 737–750, 2008.

Lanigan, G. J., Betson, N., Griffiths, H., and Seibt, U.: Carbon isotope fractionation during photorespiration and carboxylation in Senecio, Plant Physiol., 148, 2013–2020, 2008.

Le Roux, X., Bariac, T., Sinoquet H., Genty, B., Piel, C., Mariotti, A., Girardin, C., and Richard, P.: Spatial distribution of leaf water-use efficiency and carbon isotope discrimination within an isolated tree crown, Plant Cell Environ., 24, 1021–1032, 2001.

Leakey, A. D.: Rising atmospheric carbon dioxide concentration and the future of C4 crops for food and fuel, Proceedings of the Royal Society of London B: Biological Sciences, 276, 1517–2008, 2009.

Leakey, A. D., Ainsworth, E. A., Bernacchi, C. J., Rogers, A., Long, S. P., and Ort, D. R.: Elevated CO_2 effects on plant carbon, nitrogen, and water relations: six important lessons from FACE, J. Exp. Bot., 60, 2859–2876, 2009.

Lobell, D. B., Roberts, M. J., Schlenker, W., Braun, N., Little, B. B., Rejesus, R. M., and Hammer, G. L.: Greater sensitivity to drought accompanies maize yield increase in the US Midwest, Science, 344, 516–519, 2014.

Medlyn, B. E., Barton, C. V. M., Broadmeadow, M. S. J., Ceulemans, R., Angelis, P. D., Forstreuter, M., Freeman, M., Jackson, S. B., Kellomäki, S., and Laitat, E.: Stomatal conductance of forest species after long-term exposure to elevated CO_2 concentration: a synthesis, New Phytol., 149, 247–264, 2001.

Mielke, M. S., Oliva, M. A., de Barros, N. F., Penchel, R. M., Martinez, C. A., Da Fonseca, S., and de Almeida, A. C.: Leaf gas exchange in a clonal eucalypt plantation as related to soil moisture, leaf water potential and microclimate variables, Trees, 14, 263–270, 2000.

Miranda Apodaca, J., Pérez López, U., Lacuesta, M., Mena Petite, A., and Muñoz Rueda, A.: The type of competition modulates the ecophysiological response of grassland species to elevated CO_2 and drought, Plant Biolog, 17, 298–310, 2015.

Parker, W. C. and Pallardy, S. G.: Gas exchange during a soil drying cycle in seedlings of four black walnut (*Juglans nigra* l.) Families, Tree physiol., 9, 339–348, 1991.

Pons, T. L., Flexas, J., von Caemmerer, S., Evans, J. R., Genty, B., Ribas-Carbo, M., and Brugnoli, E.: Estimating mesophyll conductance to CO_2: methodology, potential errors, and recommendations, J. Exp. Bot., 8, 1–18, 2009.

Reich, P. B., Walters, M. B., and Tabone, T. J.: Response of *Ulmus americana* seedlings to varying nitrogen and water status. 2 Water and nitrogen use efficiency in photosynthesis, Tree Physiol., 5, 173–184, 1989.

Rinne, K. T., Saurer, M., Kirdyanov, A. V., Bryukhanova, M. V., Prokushkin, A. S., Churakova Sidorova, O. V., and Siegwolf, R. T.: Examining the response of larch needle carbohydrates to climate using compound-specific $\delta^{13}C$ and concentration analyses, EGU General Assembly Conference, 1814949R, 2016.

Robredo, A., Pérez-López, U., de la Maza, H. S., González-Moro, B., Lacuesta, M., Mena-Petit,e A., and Muñoz-Rueda, A.: Elevated CO_2 alleviates the impact of drought on barley improving water status by lowering stomatal conductance and delaying its effects on photosynthesis, Environ. Exp. Bot., 59, 252–263, 2007.

Robredo, A., Pérez-López, U., Lacuesta, M., Mena-Petite, A., and Muñoz-Rueda, A.: Influence of water

627   stress on photosynthetic characteristics in barley plants under ambient and elevated CO_2
628   concentrations, Biologia. Plantarum, 54, 285–292, 2010.

629   Rossmann, A., Butzenlechner, M., and Schmidt, H.: Evidence for a nonstatistical carbon isotope
630   distribution in natural glucose, Plant Physiol., 96, 609–614, 1991.

631   Streit, K., Rinne, K. T., Hagedorn, F., Dawes, M. A., Saurer, M., Hoch, G., Werner, R. A., Buchmann,
632   N., and Siegwolf, R. T. W.: Tracing fresh assimilates through *Larix decidua* exposed to elevated
633   CO_2 and soil warming at the alpine treeline using compound-specific stable isotope analysis, New
634   Phytol., 197, 838–849, 2013.

635   Tausz Posch, S., Norton, R. M., Seneweera, S., Fitzgerald, G. J., and Tausz, M.: Will intra-specific
636   differences in transpiration efficiency in wheat be maintained in a high CO_2 world? A FACE study,
637   Physiol. Plantarum, 148, 232–245, 2013.

638   Tazoe, Y., von Caemmerer, S., Estavillo, G. M., and Evans, J. R.: Using tunable diode laser spectroscopy
639   to measure carbon isotope discrimination and mesophyll conductance to CO_2 diffusion dynamically
640   at different CO_2 concentrations, Plant Cell Environ., 34, 580–591, 2011.

641   Terashima, I., Hanba, Y.T., Tazoe, Y., Vyas, P., and Yano, S.: Irradiance and phenotype: comparative
642   eco-development of sun and shade leaves in relation to photosynthetic CO_2 diffusion, J. Exp. Bot.,
643   57, 343–354, 2006.

644   Théroux-Rancourt, G., Éthier, G., and Pepin, S.: Threshold response of mesophyll CO_2 conductance to
645   leaf hydraulics in highly transpiring hybrid poplar clones exposed to soil drying, J. Exp. Bot., 65,
646   741-753, 2014.

647   Uehlein, N., Otto, B., Hanson, D. T., Fischer, M., McDowell, N., and Kaldenhoff, R.: Function of
648   Nicotiana tabacum aquaporins as chloroplast gas pores challenges the concept of membrane CO_2
649   permeability, Plant Cell, 20, 648–657, 2008.

650   Von Caemmerer, S. V. and Farquhar, G. D.: Some relationships between the biochemistry of
651   photosynthesis and the gas exchange of leaves, Planta, 153, 376–387, 1981.

652   Wall, G. W., Garcia, R. L., Kimball, B. A., Hunsaker, D. J., Pinter, P. J., Long, S. P., Osborne, C. P.,
653   Hendrix, D. L., Wechsung, F., and Wechsung, G.: Interactive effects of elevated carbon dioxide and
654   drought on wheat, Agron. J., 98, 354–381, 2006.

655   Wall, G. W., Garcia, R. L., Wechsung, F., and Kimball, B. A.: Elevated atmospheric CO_2 and drought
656   effects on leaf gas exchange properties of barley, Agr. Ecosyst. Environ., 144, 390–404, 2011.

657   Warren, C. R. and Adams, M. A.: Internal conductance does not scale with photosynthetic capacity:
658   implications for carbon isotope discrimination and the economics of water and nitrogen use in
659   photosynthesis, Plant Cell Environ., 29, 192–201, 2006.

660   Xu, D. Q.: Some problems in stomatal limitation analysis of photosynthesis, Plant Physiol. J., 33, 241–
661   244, 1997.

662   Xu, Z. and Zhou, G.: Responses of photosynthetic capacity to soil moisture gradient in perennial rhizome
663   grass and perennial bunchgrass, BMC Plant Boil., 11, 21, 2011.

664   Yang, B., Pallardy, S. G., Meyers, T. P., GU, L. H., Hanson, P. J., Wullschleger, S. D., Heuer, M.,
665   Hosman, K. P., Riggs, J. S., and Sluss D. W.: Environmental controls on water use efficiency during
666   severe drought in an Ozark Forest in Missouri, USA, Global Change Biol., 16, 2252–2271, 2010.

667   Yu, G., Wang, Q., and Mi, N.: Ecophysiology of plant photosynthesis, transpiration, and water use,
668   Science Press, Beijing, China, 2010.

669

670

Figure

1. water storage tank
2. holder
3. controller
4. soil moisture sensors
5. drip irrigation component
6. AC power supply
7. main water pipe
8. distributed water pipe
9. movable annular body
10. spindle of the annular body
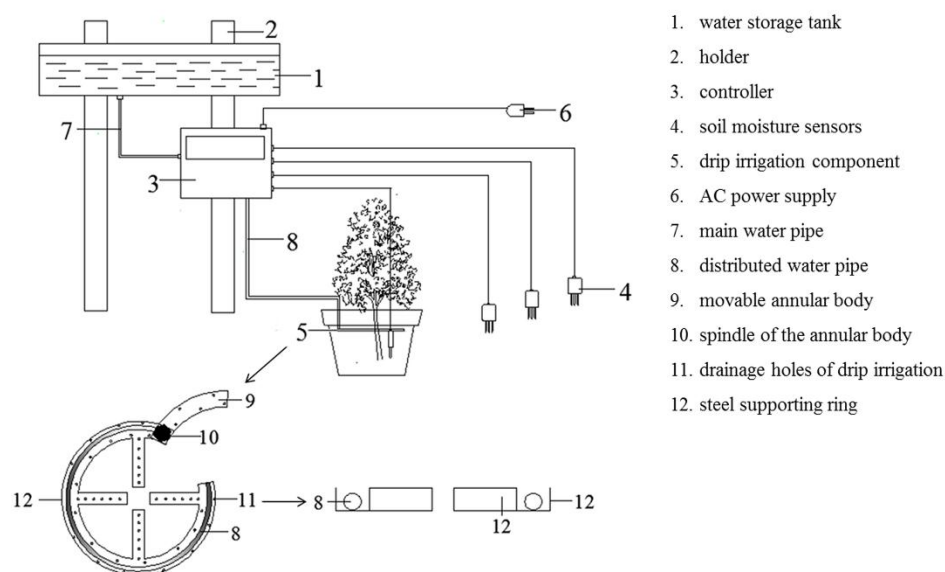11. drainage holes of drip irrigation
12. steel supporting ring

701

702 **Figure 1.** Structural diagram of the device for automatic drip irrigation

703 Arabic numerals indicate the individual parts of the automatic drip irrigation device (No. 1–7). The

704 lower-left corner of this figure presents the detailed schematic for the drip irrigation components (No. 8–

705 12). The lower-right corner of this figure shows the schematic for the drip irrigation component in profile.

706

707

708

709

710

711

712

713

714

Figure 2. Photosynthetic parameters of *P. orientalis* and *Q. variabilis* saplings in CO_2 concentrations of 400 ppm, 500 ppm, 600 ppm and 800 ppm across five soil volumetric water contents. The net photosynthetic rates (P_n, μmol m^{-2} s^{-1}), stomatal conductance (g_s, mol H_2O m^{-2} s^{-1}), intercellular CO_2 concentration (C_i, μmol CO_2 mol^{-1}), and transpiration rates (T_r, mmol H_2O m^{-2} s^{-1}) are shown in Figs. 2a and 2b, 2c and 2d, 2e and 2g, and 2g and 2h, respectively. Means $\pm$SDs, n = 32.
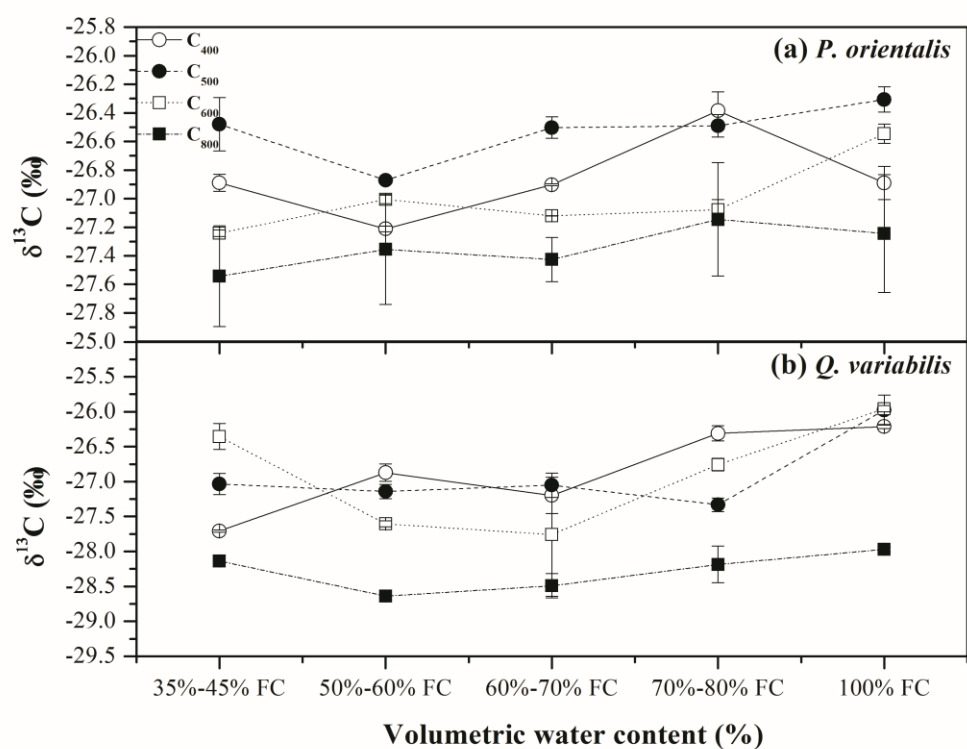
Figure 3. $\delta^{13}C$ of water-soluble compounds extracted from leaves of *P. orientalis* and *Q. variabilis* cultivated in CO_2 concentrations of 400 ppm, 500 ppm, 600 ppm and 800 ppm across five soil volumetric water contents are shown in Figs. 3a and 3b. Means $\pm$ SDs, n = 32.
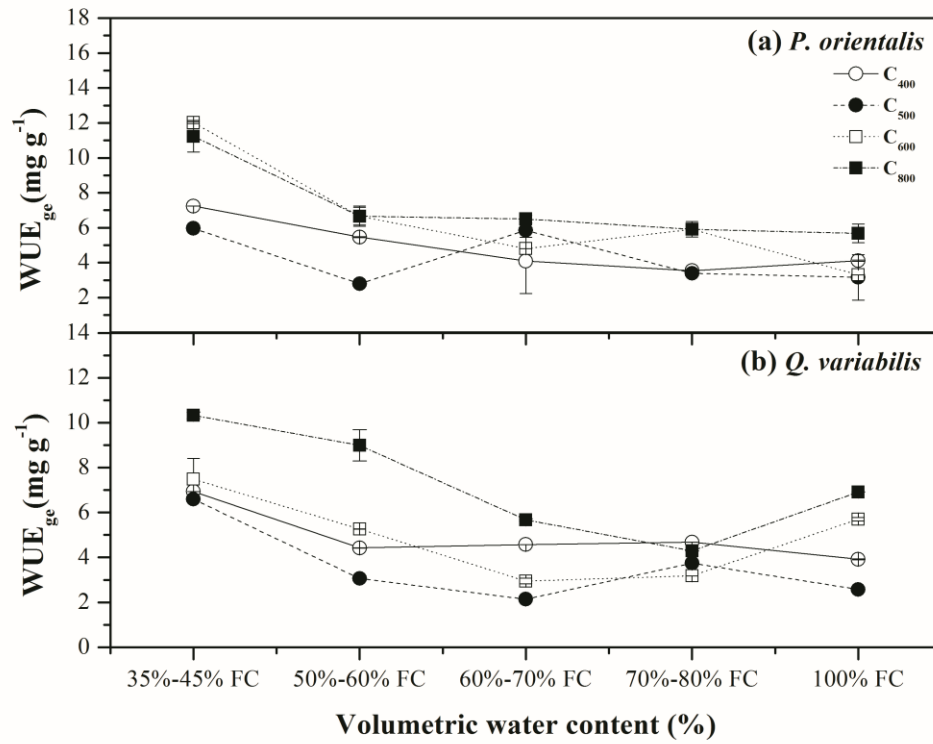
725

Figure 4. Instantaneous water use efficiency through gas exchange (WUE_{ge}) in leaves of *P. orientalis* and *Q. variabilis* cultivated in CO_2 concentrations of 400 ppm, 500 ppm, 600 ppm and 800 ppm across five soil volumetric water contents are shown in Figs. 4a and 4b. Means $\pm$ SDs, n = 32.
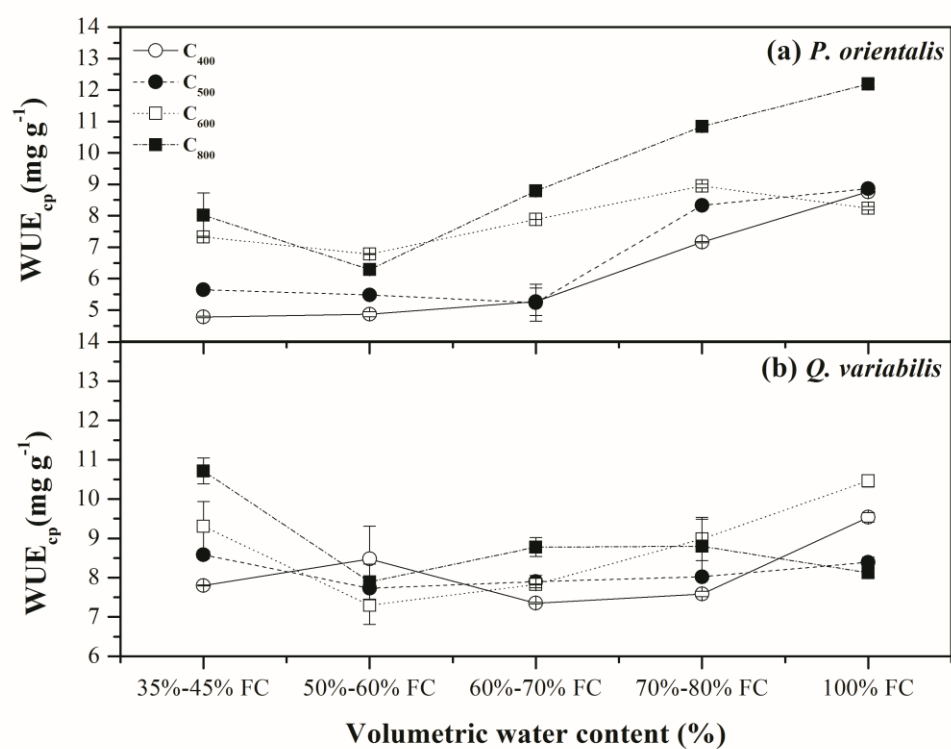
729

Figure 5. Instantaneous water use efficiency through $\delta^{13}C$ of water-soluble compounds (WUE_{cp}) in leaves of *P. orientalis* and *Q. variabilis* cultivated in CO_2 concentrations of 400 ppm, 500 ppm, 600 ppm, and 800 ppm across five soil volumetric water contents are shown in Figs. 5a and 5b. Means $\pm$ SDs, n = 32.

734

735 **Figure 6.** Variations in mesophyll conductance of *P. orientalis* and *Q. variabilis* cultivated in CO_2
736 concentrations of 400 ppm, 500 ppm, 600 ppm, and 800 ppm across five soil volumetric water contents
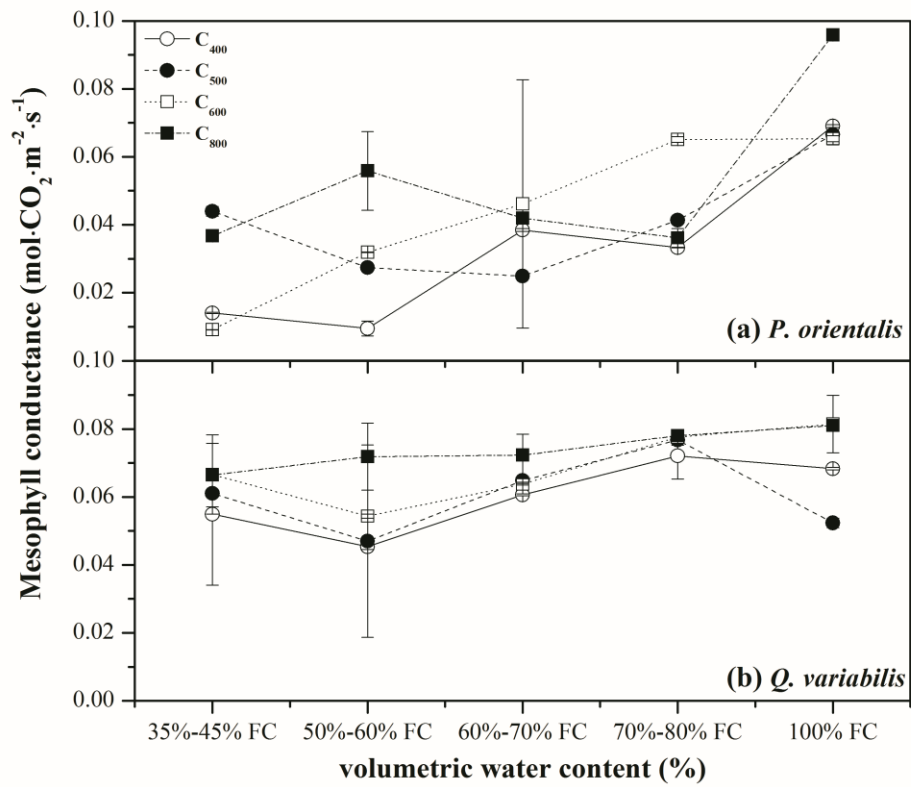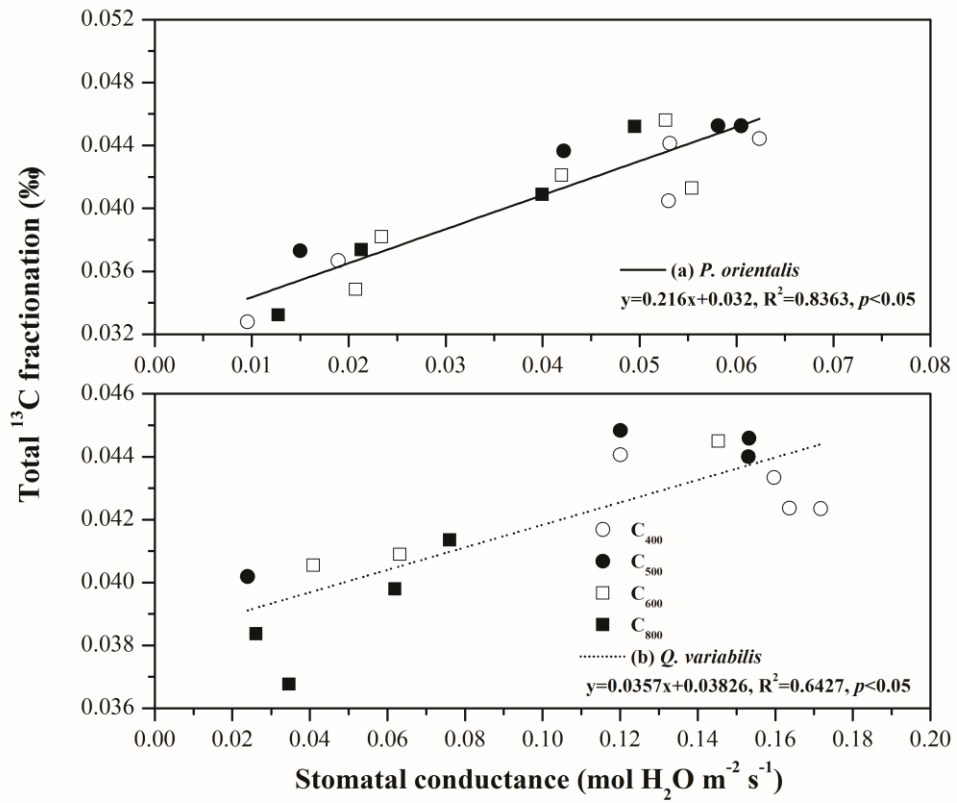737 are shown in Figs. 6a and 6b. Means ± SDs, n = 32.

738

Figure 7. Regression between stomatal conductance and total ^{13}C fractionation of *P. orientalis* and *Q. variabilis* under four CO_2 concentrations × five soil volumetric water contents are established in Figs. 7a and 7b. *p*=0.05, n = 32.
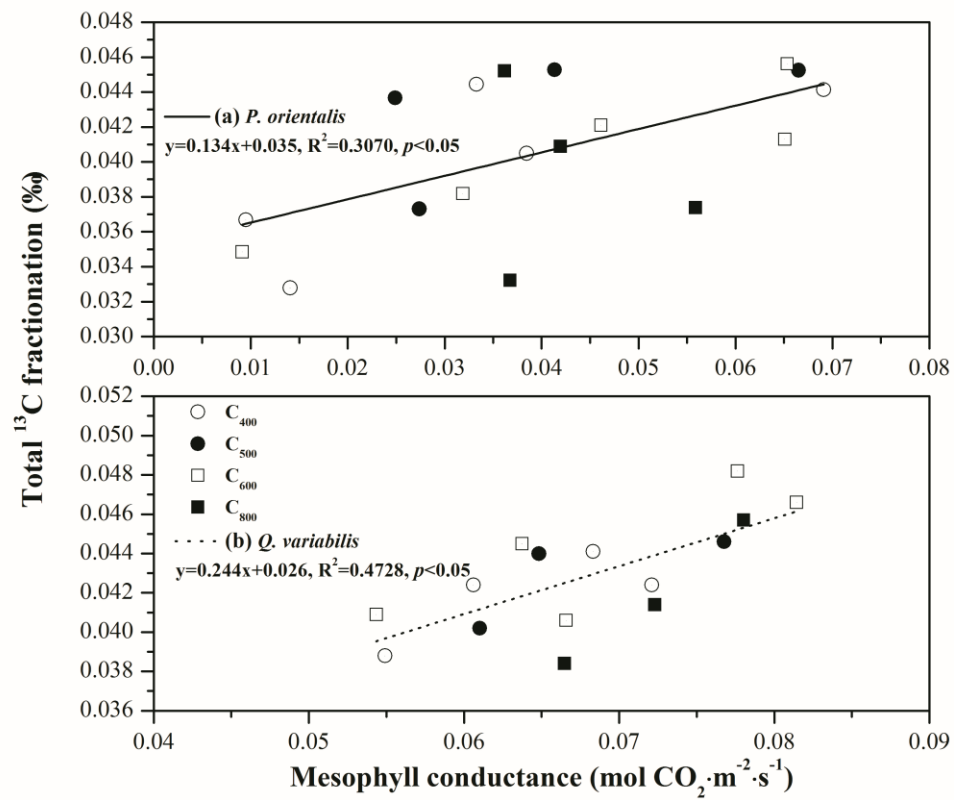
Figure 8. Regression between mesophyll conductance and total ^{13}C fractionation of *P. orientalis* and *Q. variabilis* under four CO_2 concentrations × five soil volumetric water contents are established in Figs. 8a and 8b. *p*=0.05, n = 32.

Table

747 **Table 1.** ^{13}C fractionation of *P. orientalis* and *Q. variabilis* under four CO_2 concentrations $\times$ five soil volumetric water contents.

Species	SWC (of FC)	Total ^{13}C fractionation (‰)	CO₂ concentration (ppm)				^{13}C fractionation (‰) Mesophyll conductance					^{13}C fractionation (‰) Post-photosynthesis				
			400	500	600	800		400	500	600	800		400	500	600	800
P. orientalis	35%–45%		0.0328	0.0373	0.0349	0.0332		0.0081	0.0030	0.0034	0.0072		0.0247	0.0343	0.0315	0.0260
	50%–60%		0.0367	0.0437	0.0382	0.0374		0.0018	0.0058	0.0094	0.0004		0.0349	0.0379	0.0288	0.0370
	60%–70%		0.0405	0.0366	0.0421	0.0409		0.0018	0.0050	0.0026	0.0007		0.0387	0.0316	0.0395	0.0402
	70%–80%		0.0444	0.0453	0.0413	0.0452		0.0044	0.0052	0.0103	0.0013		0.0400	0.0401	0.0310	0.0439
	100%		0.0441	0.0453	0.0456	0.0472		0.0057	0.0040	0.0025	0.0039		0.0384	0.0413	0.0431	0.0433
Q. variabilis	35%–45%		0.0388	0.0402	0.0406	0.0384		0.0007	0.0025	0.0006	0.0091		0.0381	0.0377	0.0400	0.0293
	50%–60%		0.0433	0.0448	0.0409	0.0368		0.0061	0.0084	0.0023	0.0018		0.0372	0.0364	0.0386	0.0350
	60%–70%		0.0424	0.0440	0.0445	0.0414		0.0066	0.0086	0.0078	0.0041		0.0358	0.0354	0.0367	0.0373
	70%–80%		0.0424	0.0446	0.0482	0.0457		0.0034	0.0016	0.0074	0.0028		0.0390	0.0430	0.0408	0.0429
	100%		0.0441	0.0466	0.0466	0.0398		0.0027	0.0076	0.0022	0.0125		0.0414	0.0390	0.0444	0.0273

748